



DØnote 4549-CONF

Measurement of the W Helicity in Top Quark Decays

The DØ Collaboration

URL: <http://www-d0.fnal.gov>

(Dated: August 12, 2004)

We present a search for right-handed helicity-state W -bosons in top quark events using $t\bar{t}$ decays in the e +jets and μ +jets final states. A non-zero fraction of right-handed W -bosons, f^+ , would be evidence for a V+A-current contribution to top quark decays. Using a Bayesian confidence interval, we find $0 < f^+ < 0.244$ (90% CL). This is consistent with the standard model prediction of $f^+ = 0.0$.

This is version 2.14 of the conference note.

Preliminary Results for Summer 2004 Conferences

I. INTRODUCTION

One test of the standard model (SM) is the measurement of the helicity of W -bosons in top quark decays. In the SM, the top quark decays via the V-A charged current interaction. At the Born level, this parity violating interaction limits decays of top quarks into W 's with longitudinal and left-handed helicity states with fractions f^0 and f^- respectively.

The branching ratio for f^0 is a function of the top quark mass (m_t) W -boson mass (M_W), and b -quark mass [1]. The effects of the b -quark mass are small and hence:

$$f^0 \approx \frac{m_t^2}{m_t^2 + 2M_W^2} \quad (1)$$

With the present measured values of the top quark and W -boson mass the SM prediction gives $f^0 = 0.701 \pm 0.016$ and $f^- \approx 0.30$. There are almost no decays into right-handed W helicity states ($f^+ = 0.0$) since the b -quark helicity in this case would necessarily be right-handed and hence greatly suppressed. The helicity states for antitop decays would be reversed from those given above. An early theoretical treatment of top quark decays is given in [2]. In this measurement we search for a non-zero value of f^+ that would be evidence for a possible V+A admixture to the $t \rightarrow b$ current. In the context of this model, f^0 is fixed at the standard model value.

In Run I of the Tevatron, CDF measured $f^+ = 0.11 \pm 0.15$ and $f^0 = 0.91 \pm 0.37 \pm 0.13$ [3]. DØ obtained $f^0 = 0.56 \pm 0.31$ [4, 5]. In addition to direct measurements, data on $b \rightarrow s\gamma$ decays have been used to set a limit on W_R and W_L mixing [6, 7].

Our analysis consists of selecting events using nearly the same criteria used by the Winter 2004 lepton+jets $t\bar{t}$ production cross section analyses [8]. One exception is that we do not reject events that contain jets that are tagged with soft muons. In addition we also employ topological criteria to increase the expected number of signal versus background.

For events passing all selection criteria we perform a constrained kinematic fit to select the b -jet associated with the leptonic W . We use the term “leptonic W ” as shorthand notation for the phrase “ W that decays leptonically”. In the very small percentage of cases where the kinematic fit does not converge, we use a simpler χ^2 method to select the b -jet associated with the leptonic W . Both methods use the measured top mass and W -boson mass as constraints.

Once the b -jet associated with the leptonic W is identified we calculate $\cos\theta^*$. We define $\cos\theta^*$ as the cosine of the angle between the lepton momentum and the initial W -boson momentum when boosted to the rest frame of the leptonic W . With this definition, the $\cos\theta^*$ distribution for right-handed W 's is peaked towards $\cos\theta^* = +1$. We use the object momenta returned from the kinematic fit in calculating $\cos\theta^*$.

We produce templates in $\cos\theta^*$ for $t\bar{t}$ signal assuming different V+A fractions f^+ and for $Wjjjj$ and “QCD” backgrounds. We rely on Monte Carlo to produce the different $\cos\theta^*$ distributions except for the multijet background (called “QCD”), which is taken from data.

We use these templates in a binned likelihood fit to find the V+A fraction f^+ given by the data. The resulting log likelihood curves are interpreted using both Bayesian and frequentist approaches. We also use these templates in fits to ensembles of Monte Carlo events in order to test the veracity of our procedure and to estimate systematic uncertainties.

II. EVENT SELECTION

This analysis is based on 168.7 pb^{-1} of e +jets data and 158.4 pb^{-1} of μ + jets data accumulated by DØ during Run II of the Tevatron. We also use Monte Carlo samples of events generated by ALPGEN [9] or PYTHIA [10].

Our preselection criteria for the μ +jets and e +jets channels are given in Tables I and II respectively. These criteria are identical to those used in the $t\bar{t}$ production cross section analysis for Winter 2004 conferences, except we do not reject events in which a soft muon is associated with a jet.

Our final selection criteria are the preselection criteria plus a topological criterion used to further increase the expected ratio of $S/\sqrt{S+B}$. Presently we use a cut on a six-variable topological likelihood L_t given in Table III. The topological likelihood variables and cut value were optimized by performing ensemble tests and choosing a definition and cut that minimized the average width of the 68% Bayesian confidence interval for the measurement of f^+ .

The topological likelihood L_t is based on six kinematic variables, defined as follows:

- Aplanarity \mathcal{A} , defined as 3/2 times the smallest eigenvalue of the normalized momentum tensor of the jets and lepton. \mathcal{A} is a measure of the deviation from flatness of the event, and $t\bar{t}$ events tend to have larger values than background events.

Selection Cut
≥ 3 tracks at the primary event vertex (PV)
$ Z_{PV} < 60$ cm
$\geq 1 \mu$
Only 1 isolated μ
Highest $P_T^\mu > 20$ GeV
Muon track passes within 3σ of PV
$ \Delta z(\mu, PV) < 1$ cm
≥ 4 jets
4 jets with $P_T > 15$ GeV
$\Delta R(\mu, jet) > 0.5$
$\cancel{E}_T > 17$ GeV
$1.2 - 0.03 \times \cancel{E}_T [\text{GeV}] < \Delta\phi(\mu, \cancel{E}_T) < 1.3 + 0.08 \times \cancel{E}_T [\text{GeV}]$
$\Delta\phi(\text{leadingjet}, \cancel{E}_T) < 2.2 + 0.04 \times \cancel{E}_T [\text{GeV}]$
μ +jets trigger requirement
Isolated muon is the highest P_T muon

TABLE I: Preselection criteria for the μ +jets channel

Selection Cut
≥ 3 tracks at the vertex
$ Z_{\text{vertex}} < 60$ cm
≥ 1 electron
Only 1 electron with $P_T^e > 15$ GeV
EM likelihood > 0.75 (we sometimes call this “isolated”)
Electron has matched track
Electron $P_T > 20$ GeV
$\eta_{\text{detector}}^e < 1.1$
$ \Delta z(e, PV) < 1$ cm
≥ 4 jets
4 jets with $P_T > 15$ GeV
$\cancel{E}_T > 20$ GeV
$\Delta\phi(e, \cancel{E}_T) > 1.7 + 0.02 \times \cancel{E}_T [\text{GeV}]$
e +jets trigger requirements
Isolated electron is the highest P_T electron

TABLE II: Preselection criteria for the e +jets channel

Cut	μ +jets	e +jets
L_t	> 0.60	> 0.60

TABLE III: Topological cut on L_t (choice 2) used in the final selection criteria.

- H_{T2}^l , defined as the sum of the E_T 's of all the jets in the event except the highest- E_T one, divided by the sum of the magnitudes of the longitudinal momenta of the jets, lepton, and neutrino (p_z of the neutrino is calculated using a W mass constraint). Top quark events will tend to be more central and thus have higher values of H_{T2}^l .
- $K_{T\text{min}}^l$, defined as the distance in $\eta - \phi$ space between the closest pair of jets multiplied by the E_T of the lowest- E_T jet in the pair, and divided by the E_T of the W . Only the four leading- E_T jets are considered in computing this variable. Jets arising from gluon radiation (as is the case for background) will tend to result in low values of $K_{T\text{min}}^l$.
- Sphericity \mathcal{S} is defined as $3/2$ times the sum of the two smallest eigenvalues of the normalized momentum tensor of the jets in the event. This variable is similar to \mathcal{A} , and $t\bar{t}$ events will tend to have larger values than background.
- H_T , defined as the scalar sum of all jet P_T values > 15 GeV. Jets arising from gluon radiation in general have lower P_T than jets in $t\bar{t}$ events so background events will tend to have smaller values of H_T compared to signal events.
- Kinematic fit χ^2 , defined as the χ^2 associated with a kinematic fit to the hypothesis of $t\bar{t}$ decays in the e +jets or μ +jets final states. Signal events will naturally have smaller χ^2 values than background events.

The efficiency of topological likelihood cut as a function of f^+ is shown in Figure 1. There is a slight variation in efficiency that we later account for as a systematic error in the selection efficiency. The nominal efficiency we use for $t\bar{t}$ events is taken from the $f^+=0.15$ sample.

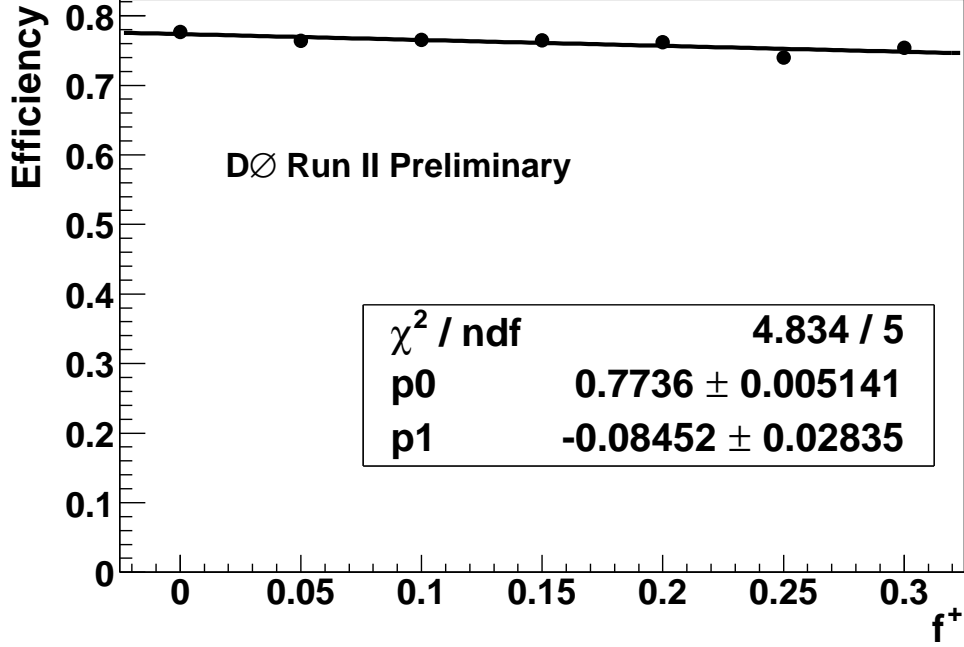


FIG. 1: Efficiency of the topological likelihood cut as a function of f^+ .

The fact that we are using Monte Carlo distributions as input to the topological likelihood L_t raises the question of how well data distributions agree with the Monte Carlo. We compare data and Monte Carlo distributions for preselected events for the transformed variables aplanarity, sphericity, $K'_{T\min}$, H_T , and kinematic fit χ^2 . We also compare data and Monte Carlo distributions for preselected events for \cancel{E}_T , $P_T^\mu(\text{highest})$, and $P_T^{jet}(\text{highest})$. There is relatively good agreement between data and Monte Carlo in all distributions.

III. SIGNAL AND BACKGROUND DETERMINATION

We use lepton selection efficiencies measured in data, and the topological selection efficiency measured in Monte Carlo, to determine the number of signal and background events in the selected data. Below we use the terms “loose”, “preselected”, and “selected” events. Preselected events are those events that pass the selection criteria in Table I and Table II. Loose events are those events that pass the preselection criteria except the isolation criterion. Specifically, N_{loose} in the μ +jets channel is the number of events passing all preselection criteria except for the muon isolation criterion. N_{loose} in the e +jets channel is the number of events passing all preselection criteria except for the EM likelihood criterion. Selected events are those events that pass the preselection cuts and the topological likelihood cut. At total of 31 μ +jets and 49 e +jets events passed all selection criteria.

Equation 2 is used to determine the number of $t\bar{t} + Wjjjj$ ($N_{pre}^{t\bar{t}+W}$) and QCD(N_{pre}^{QCD}) events after preselection but before applying the topological likelihood cut. $N_{pre}^{t\bar{t}+W}$ and N_{pre}^{QCD} are estimated as follows:

$$N_{pre}^{t\bar{t}+W} = \frac{N_{pre} - \epsilon_{QCD} N_{loose}}{\epsilon_{sig} - \epsilon_{QCD}} \quad \text{and} \quad N_{pre}^{QCD} = \frac{\epsilon_{sig} N_{loose} - N_{pre}}{\epsilon_{sig} - \epsilon_{QCD}}, \quad (2)$$

where ϵ_{sig} is the efficiency for both $t\bar{t}$ and $Wjjjj$. The inputs to Eq. (2) are given in Table IV. The output from Eq. (2) is given in Table V. The efficiencies and their errors are determined using a low-missing- E_T control sample for QCD and a $Z \rightarrow \mu\mu$ sample for isolated muons, as detailed in the production cross section note for the lepton plus jets decay channel [8]. N_{loose} and N_{pre} were defined in the first paragraph of this section.

Quantity	μ +jets	e +jets
N_{loose}	250	355
N_{pre}	118	160
ε_{sig}	0.819 ± 0.018	0.876 ± 0.010
ε_{QCD}	0.075 ± 0.023	0.082 ± 0.015

TABLE IV: Inputs to Eq. (2)

Quantity	μ +jets	e +jets
$N_{pre}^{t\bar{t}+W}$	109.3 ± 11.8	144.4 ± 13.3
N_{pre}^{QCD}	8.7 ± 1.4	15.6 ± 1.6

TABLE V: Outputs from Eq. (2)

Quantity	μ +jets	e +jets
N_{pre}	118	160
N_{sel}	31	49
$\varepsilon_{t\bar{t}}$	0.743 ± 0.023	0.792 ± 0.014
ε_{Wjjjj}	0.187 ± 0.010	0.182 ± 0.010
ε_{QCD}	0.244 ± 0.038	0.175 ± 0.027

TABLE VI: Inputs to Eqs.(3) and (4)

Source	μ +jets	e +jets
$t\bar{t}$	11.3 ± 1.3	25.9 ± 1.5
$Wjjjj$	17.6 ± 1.2	20.3 ± 1.5
QCD	2.1 ± 0.5	2.7 ± 0.5

TABLE VII: Outputs from Eqs.(3) and (4)

We use Eqs. (3) and (4) in order to determine the number of signal and background events in our final sample after all selection criteria. The equations solved are:

$$N_{sel}^{t\bar{t}} \equiv \varepsilon_{sel}^{t\bar{t}} N_{pre}^{t\bar{t}} = \varepsilon_{sel}^{t\bar{t}} \frac{N_{sel} - \varepsilon_{sel}^W N_{pre} - (\varepsilon_{sel}^{QCD} - \varepsilon_{sel}^W) N_{pre}^{QCD}}{\varepsilon_{sel}^{t\bar{t}} - \varepsilon_{sel}^W} \quad (3)$$

$$N_{sel}^W = \varepsilon_{sel}^W N_{pre}^W = \varepsilon_{sel}^W \frac{N_{sel} - \varepsilon_{sel}^{t\bar{t}} N_{pre} + (\varepsilon_{sel}^{t\bar{t}} - \varepsilon_{sel}^{QCD}) N_{pre}^{QCD}}{\varepsilon_{sel}^W - \varepsilon_{sel}^{t\bar{t}}} \quad (4)$$

The quantities input to Eqs. (3) and (4) and their errors for the μ +jets and e +jets channels are given in Table VI.

For $t\bar{t}$ events we calculate $\varepsilon_{sel}^{t\bar{t}}$ using the $f^+=0.15$ Monte Carlo sample. This minimizes the error due to the variation of the L_t efficiency as a function of f^+ . The variation in the efficiency as a function of f^+ (Figure 1) is included in the error for $\varepsilon_{sel}^{t\bar{t}}$ listed in Table VI.

The number of $t\bar{t}$, $Wjjjj$ and QCD events resulting from Eqs. (3) and (4) are given in Table VII. We use these numbers of signal and background events to perform ensemble tests and as input into our likelihood used to determine f^+ . The uncertainties in these numbers include the uncertainty in the topological likelihood selection efficiency, which varies as a function of f^+ .

IV. TEMPLATES

The input to the maximum likelihood fit requires templates of signal and backgrounds. The $t\bar{t}$ and $Wjjjj$ templates are generated using the Monte Carlo samples described in Section II. The $t\bar{t}$ templates are produced for f^+ values from 0.0 to 0.3 in steps of 0.05. The events are required to pass all selection cuts.

The QCD templates are found using data. To define the QCD sample, the events are required to pass all selection cuts with one with some of the lepton criteria inverted. In the μ +jets channel we define a QCD sample by requiring

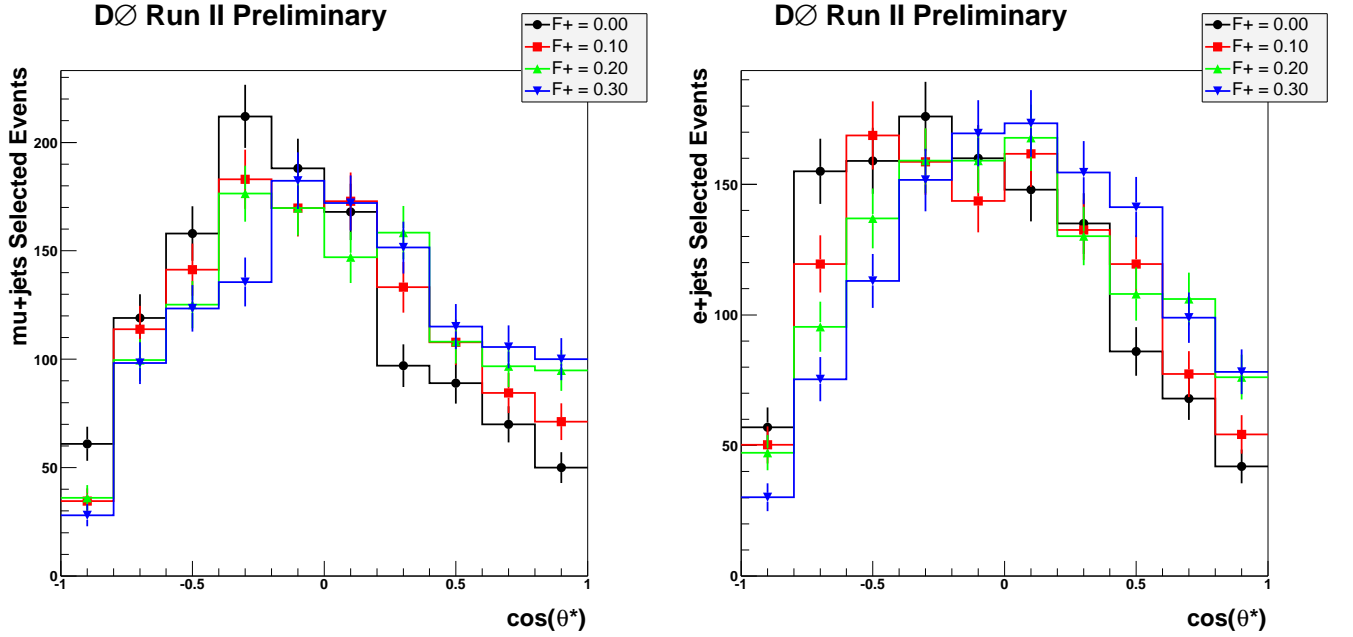


FIG. 2: $\cos\theta^*$ distribution for μ +jets (left), e +jets (right) $t\bar{t}$ signal for $f^+=0.0, 0.10, 0.20, 0.30$

the high P_T muon not be isolated. In the e +jets channel we define a QCD sample by requiring the high P_T electron not to pass the EM likelihood cut.

The $\cos\theta^*$ templates used in the maximum likelihood fit are shown in Fig. 2, first for the μ +jets channel, then for the e +jets channel. The events pass all selection criteria.

In order to study certain systematic errors we also make templates varying the top quark mass and the jet energy scale corrections.

When used in the maximum likelihood fit, the templates are rebinned to have five bins. We chose five bins since based on a study of ensemble tests in which the number of bins was varied from 2 to 50, in which we found that using five bins gave a reasonable combination of sensitivity and stability.

Our templates were produced using a constrained kinematic fit to the $t\bar{t}$ hypothesis with the top mass fixed to 175 GeV to determine the b -jet associated with the leptonic W . The object momenta returned from the constrained kinematic fit are used in the calculation of $\cos\theta^*$. In the cases where the kinematic fit failed to converge we employed a simpler χ^2 method that compares the calculated and known hadronic and leptonic decay top quark masses and hadronic W mass to select the b -jet, and used the object momenta measured prior to the constrained kinematic fit in calculating $\cos\theta^*$. However these cases are a rare circumstance, occurring in about 0.5% of events.

The nominal jet energy scale corrections were applied to both data and Monte Carlo. The nominal parton and eta-dependent correction were used in selecting the b -jet associated with the leptonic W (either with the constrained kinematic fit or the simpler χ^2 method).

V. MAXIMUM LIKELIHOOD FIT

We perform a binned maximum likelihood fit to extract the value of f^+ , the fraction of V+A in the top decay, most consistent with the data. As input to the fit we have the distributions of $\cos\theta^*$ in: the selected data events, ALPGEN $t\bar{t}$ Monte Carlo with $f^+ = 0.00, 0.05, 0.10, 0.15, 0.20, 0.25$, and 0.30, ALPGEN $Wjjjj$ Monte Carlo, and QCD background from data. We also note in the ALPGEN V+A samples, the fraction f^0 is constant (70%) for all samples.

For each f^+ value, we compute the likelihood of the data to be consistent with the sum of signal and background templates. The likelihood is computed by multiplying the Poisson probabilities of each template bin being consistent with the data, using a method in which the finite template statistics are explicitly accounted for [11]. We also have a prior expectation for the normalization of the background, which is expressed with a Gaussian term in the likelihood. We define the likelihood as

$$L(f^+) = \prod_{i=1}^{N_{\text{bkg}}} e^{(n_{b,i} - \overline{n_{b,i}})^2 / 2\sigma_{b,i}^2} \times \prod_{j=1}^{N_{\text{bins}}} P(d_j; n_j) \times \prod_{k=0}^{N_{\text{sources}}} B(a_{jk}; A_{jk}, p_k), \quad (5)$$

where $P(x; y)$ is the Poisson probability for x events given an average value y and $B(m; n, p)$ is the binomial probability for observing m events out of n possible given probability p .

In the Gaussian term, N_{bkg} is the number of background sources ($Wjjjj$ and QCD in this analysis), $\overline{n_{b,i}}$ is the observed number of events for the i th background, $\sigma_{b,i}$ is the systematic uncertainty on the observed number, and $n_{b,i}$ is the expected number of events for the i th background. In the Poisson term, d_j is the number of data events in the j th bin of the $\cos\theta^*$ distribution and n_j is the predicted number of signal and background events in the j th bin of the distribution. In the binomial term, a_{jk} is the actual number of Monte Carlo signal and background events in the j th template bin, A_{jk} is the (unknown) expected number of Monte Carlo signal and background events in the j th template bin and p_k is the probability for observing the k th source ($t\bar{t}$, $Wjjjj$ and QCD). To be precise, $p_k = n_k/N_k$ where n_k is the number of events from a given source in the data sample, and N_k is the number of entries in the template used to model that source.

We minimize the $-\ln L$ for each trio of templates (two background templates and one f^+ template) (the a_{jk}) and data distribution (the d_j). The minimization is with respect to the n_k and the expected number of Monte Carlo (template) signal and background events A_{jk} . The procedure is simplified by performing the minimization of the A_{jk} analytically. The result of the fit then gives the predicted number of events in each bin n_j .

To summarize, we minimize $-\ln L$ using the likelihood given above. However when comparing values of the likelihood at each value of f^+ we take the value of $-\ln L$ to be that using only the Gaussian and Poisson terms. This prescription still accounts for finite template statistics but removes the correlation between L and the template statistics. The result is a distribution of $-\ln L$ points versus f^+ . We fit these points to a parabola to estimate the likelihood as a function of f^+ .

In the event that multiple channels enter the fit (e +jets and μ +jets in this case) the $-\ln L$ points are calculated as described above for each channel separately, then summed. A parabola is fit to the summed points to determine the overall likelihood as a function of f^+ .

Since in our assumed model f^+ must lie between 0 and 0.30, we use a Bayesian technique to determine a 68% CL range for the true value of f^+ . We choose to use a prior probability that is flat in the physically-allowed region of f^+ , and zero elsewhere. With this choice, finding a Bayesian confidence interval is equivalent to integrating the likelihood curve. If the parabola fit to the $-\ln L$ points has its minimum in the allowed range, we take the value of that minimum (i.e. the maximum of L) as the most likely value x_{ML} . We then find the points x_{min} and x_{max} such that:

$$\frac{\int_{x_{\text{min}}}^{x_{\text{ML}}} L(x) dx}{\int_0^{0.30} L(x) dx} = \frac{\int_{x_{\text{ML}}}^{x_{\text{max}}} L(x) dx}{\int_0^{0.30} L(x) dx} = 0.34$$

If x_{ML} lies outside the allowed range (or close enough to the boundary that the x_{max} or x_{min} cannot be found by both equations above), a single-sided range is reported:

$$\frac{\int_{x_{\text{min}}=0.0}^{x_{\text{max}}} L(x) dx}{\int_0^{0.30} L(x) dx} = 0.68 \quad \text{or} \quad \frac{\int_{x_{\text{min}}}^{x_{\text{max}}=0.30} L(x) dx}{\int_0^{0.30} L(x) dx} = 0.68$$

If x_{ML} is less than (or close to) 0.0, then $x_{\text{min}} = 0$ and x_{max} is calculated. If x_{ML} is greater than (or close to) 0.30, then $x_{\text{max}} = 0.30$ and x_{min} is calculated. Thus in all cases there is both an x_{min} and x_{max} .

In the case where the $-\ln L$ points form an “upside-down” parabola, x_{ML} is taken to be at the physical boundary ($f^+ = 0.0$ or 0.30) with the smallest value of $-\ln L$.

VI. RESULTS FROM ENSEMBLE TESTS

We test the performance of the maximum likelihood fit by means of Monte Carlo ensemble tests. For these tests, we assume a true value of f^+ and form a mock data set by drawing events from the appropriate Monte Carlo samples. Each data set so formed has the same number of μ +jets and e +jets as we observe in the real data sample (Table VII), but the number of signal and background is varied according to the binomial distribution. (Also once the number of

True f^+	Ave. Bayesian result	Ave. size of 68% CL range	Fraction in 68% CL range	Fraction with good parabolas
0.00	0.07	0.16	0.697	0.704
0.05	0.12	0.17	0.590	0.822
0.10	0.12	0.17	0.692	0.794
0.15	0.15	0.17	0.817	0.867
0.20	0.18	0.17	0.711	0.868
0.25	0.20	0.17	0.697	0.863
0.30	0.21	0.16	0.633	0.819

TABLE VIII: Results of Monte Carlo ensemble tests on mock data samples that model the current real data sample. The results in this table are for $\cos\theta^*$ templates having five bins.

Source	Uncertainty
Top mass	0.11
Jet energy scale	0.04
W + jets model	0.08
$t\bar{t}$ model	0.05
Total	0.15

TABLE IX: Summary of the systematic errors on f^+ .

background events in a particular mock data set is determined, the number of $Wjjjj$ and QCD events is allowed to fluctuate binomially as well).

The mock data set is then fit according to the same procedure used for fitting the real data. By repeating the process 1000 times we can investigate the statistical properties of the maximum likelihood fit. The results are given in Table VIII. Note that while the general trend is reasonable (the average of the most likely value of f^+ increases as the true f^+ increases), the change in the average result is much less than the change in true f^+ . The fact that the average Bayesian result is not in general equal to the true f^+ value is a byproduct of the fact that the results are constrained to the physical range, and does not reflect a systematic bias in the analysis.

Also shown in the table is the average size of the 68% confidence interval (CL) and the fraction of times in which the 68% CL range contains the true value of f^+ . Note the average size of the 68% CL is slightly over half the allowed range of f^+ . The fact that the fraction of times in which the 68% CL contains the true f^+ value is 82% for $f^+=0.15$ is a reflection of this average size. Both the fraction of times in which the 68% CL contains the true value of f^+ and the fraction of times there is a good parabola are symmetric about $f^+=0.15$, as expected. These ensemble tests show that the Bayesian confidence interval behaves properly. When one averages over all possible values of f^+ , the probability for the true f^+ to be in the 68% Bayesian confidence interval is 69.1%, which is reasonable agreement with expectation.

VII. STATISTICAL AND SYSTEMATIC ERRORS

Statistical uncertainties in both the data and templates are handled by the likelihood fit using Poisson statistics for the data and binomial statistics for the templates.

Sources of systematic errors arise from the uncertainties in the top mass, jet energy scale, and Monte Carlo models of signal and background. Variations in these parameters can change the measurement in two ways: by altering the estimate of the background in the final sample (i.e., if the final selection efficiency changes) and by modifying the shape of the $\cos\theta^*$ templates.

We estimate the magnitude of these uncertainties by running ensemble tests using the standard templates, but with the mock data drawn from samples with the appropriate parameter varied. The signal and background content of the ensembles is fixed to the values we expect using our nominal final selection efficiencies, but the background constraint input to the maximum likelihood fit is varied to reflect the shifted final selection efficiency. The results are summarized in Table IX, and details of the calculations are given below.

To estimate the systematic error due to the uncertainty of the top quark mass we use $f^+=0.0$ samples with the top quark mass set to 170, 175, and 180 GeV.

The jet energies against which the selection criteria are applied contain the nominal jet energy scale corrections. Additionally, we apply parton and eta dependent corrections to these jet energies when calculating $\cos\theta^*$.

To estimate the systematic error due to the uncertainty of the jet energy scale we vary the jet energy scale by $\pm 1\sigma$ about the nominal value. The nominal value is used to correct jets back to the particle level energy and to equate

Result for f^+	CL
$0 < f^+ < 0.131$	68%
$0 < f^+ < 0.236$	90%
$0 < f^+ < 0.253$	95%

TABLE X: Bayesian result for f^+ for various confidence levels. This result includes statistical errors only.

the energy scales of jets in data and Monte Carlo. To estimate the systematic error due to the uncertainty of the jet energy scale we first modify the jet energies to have the values given by varying the jet energy scale by $\pm 1\sigma$. The missing E_T is then adjusted to account for changes in the relevant components of the jet scale shift (e.g. missing E_T is changed to reflect uncertainty in hadronic response, but not uncertainty in out-of-cone showering). We use these new jet energies and missing E_T when applying the selection criteria. Next we apply parton and eta dependent corrections to the uncorrected jet energies, but now vary these parton and eta dependent corrections by $\pm 1\sigma$. The parton and eta dependent corrections are used to correct the energy of the jet to that of the original parton. We then calculate $\cos\theta^*$ using these jet energies within the constrained kinematic fit.

Another source of systematic uncertainty is the model of the $Wjjjj$ background. We tested this by comparing the results using ALPGEN samples generated with different factorization scales.

Finally we consider the model of $t\bar{t}$ decays. As an alternative to the nominal ALPGEN $t\bar{t}$ sample, we generate PYTHIA samples of $t\bar{t}$ in the μ +jets decay channel, passed through a parton-level selection such that the surviving events have a $\cos\theta^*$ distribution identical to that expected for purely right-handed, longitudinal, or left-handed W 's. We then combine these three separate sets of events in the correct proportions to mimic any given f^+ value.

VIII. RESULTS FROM DATA

The results of applying our maximum likelihood fit to the $\cos\theta^*$ distribution observed in the data are shown in Figure 3 for μ +jets events, Figure 4 for e +jets events, and Figure 5 for the combined data sample. The parabola that best fits the combined $-\ln L$ points has a minimum outside the physically-allowed region (at $f^+ = -0.105 \pm 0.188$). The Bayesian confidence intervals for different confidence levels are given in Table X. This result includes statistical errors only.

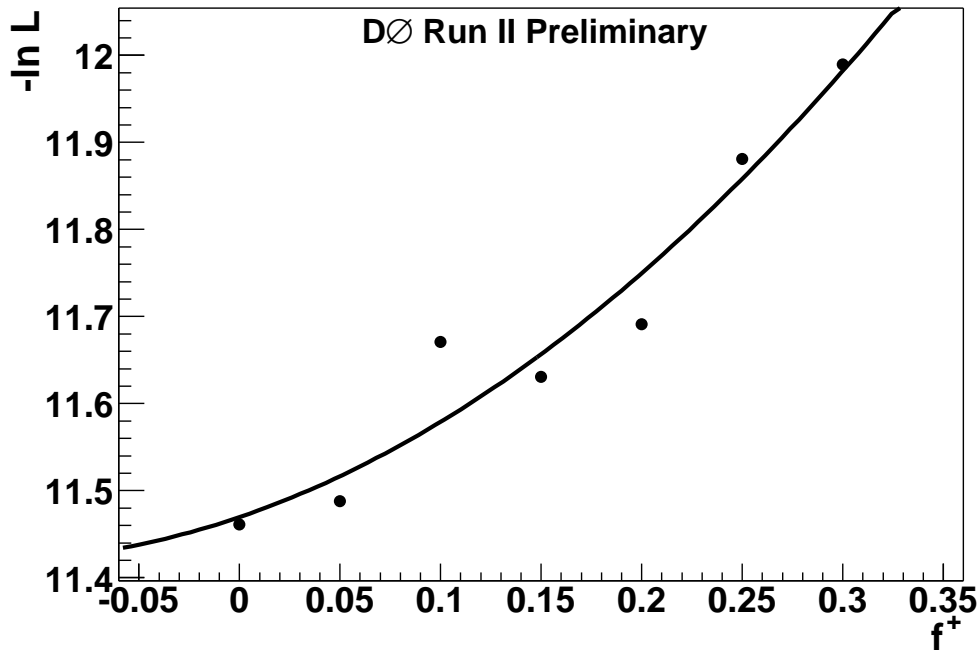


FIG. 3: Result of the maximum likelihood fit for f^+ on the μ +jets data.

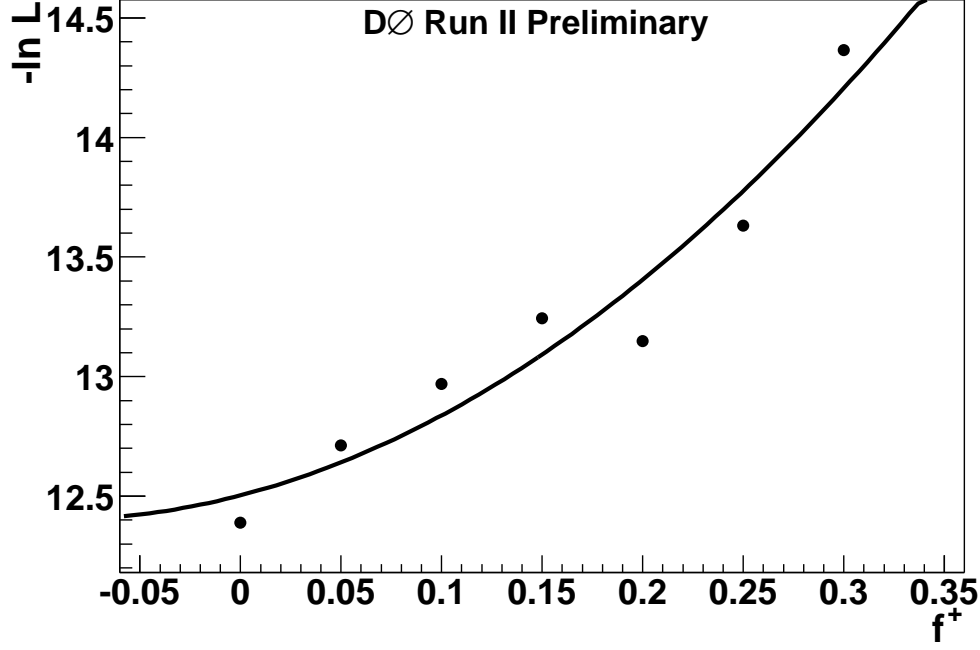


FIG. 4: Result of the maximum likelihood fit for f^+ on the e +jets data.

Signal Model	μ +jets		e +jets	
f^+	$t\bar{t}$	$Wjjjj$ +QCD	$t\bar{t}$	$Wjjjj$ +QCD
0.00	10.0	19.8	25.3	23.1
0.05	10.0	19.8	24.6	23.1
0.10	9.3	19.9	24.3	23.1
0.15	9.3	19.9	23.7	23.2
0.20	9.1	19.9	23.7	23.2
0.25	8.3	19.9	22.8	23.3
0.30	8.0	19.9	21.3	23.4

TABLE XI: Number of signal and background events resulting from the best fit using each f^+ signal model

Result for f^+	CL
$0 < f^+ < 0.159$	68%
$0 < f^+ < 0.244$	90%
$0 < f^+ < 0.267$	95%

TABLE XII: Bayesian result for f^+ for various confidence levels. This result includes both statistical and systematic errors.

We also show plots comparing the data distribution to the best fit model ($f^+ = 0.0$). In Fig. 6-8 the data is shown as the points with error bars, the best fit signal template as the dashed histogram, the best fit background template as the dotted histogram, and the sum as the solid histogram. The best fit templates are normalized according to the fitted signal and background levels at the best fit f^+ point (0.0 in our case).

We also give the number of signal and background events resulting from the best fit using each f^+ signal model (Table XI).

The systematic errors in the last section are included in the fit by convoluting a Gaussian function with a width given by the total systematic error with the Gaussian resulting from the maximum likelihood fit. The results including systematic errors for different confidence levels are given in Table XII. The maximum likelihood distribution including statistical errors and including both statistical and systematic errors is shown in Figure 9. These results are interpreted as, for any one experiment, there is a x% chance that the true value of f^+ lies within the x% confidence interval.

The standard model (SM) value of $f^+ = 0$ is consistent with our results, but increased data and Monte Carlo statistics will be required to rule out any non-SM value.

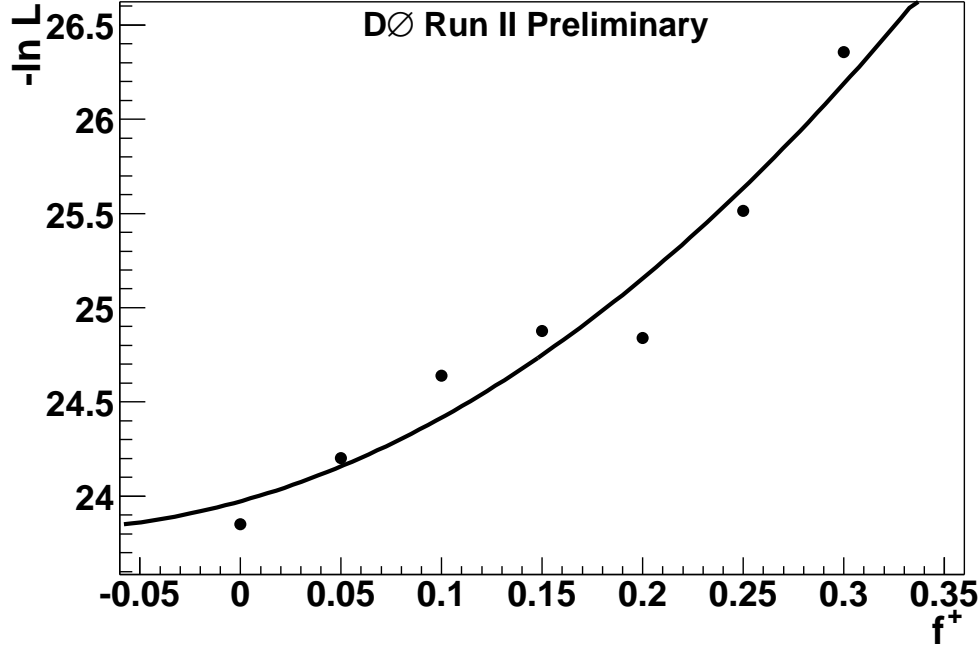


FIG. 5: Result of combining the e +jets and μ +jets maximum likelihood fits.

IX. CONCLUSIONS

We have measured the fraction of right-handed W 's (f^+) in top decays using the lepton plus jets decay channels. Using a Bayesian interpretation for confidence intervals and including both statistical and systematic uncertainties we find

$$0 < f^+ < 0.244 \text{ (90\% CL)}$$

This means, for any one experiment, there is a 90% chance that the true value of f^+ lies within the 90% confidence interval.

We have also performed a frequentist analysis based on Feldman-Cousins [12] that gives a similar result. This measurement is in agreement with the Standard Model prediction of $f^+ = 0.0$.

Acknowledgments

We thank the staffs at Fermilab and collaborating institutions, and acknowledge support from the Department of Energy and National Science Foundation (USA), Commissariat à L'Energie Atomique and CNRS/Institut National de Physique Nucléaire et de Physique des Particules (France), Ministry for Science and Technology and Ministry for Atomic Energy (Russia), CAPES, CNPq and FAPERJ (Brazil), Departments of Atomic Energy and Science and Education (India), Colciencias (Colombia), CONACyT (Mexico), Ministry of Education and KOSEF (Korea), CONICET and UBACyT (Argentina), The Foundation for Fundamental Research on Matter (The Netherlands), PPARC (United Kingdom), Ministry of Education (Czech Republic), Natural Sciences and Engineering Research Council and West-Grid Project (Canada), BMBF (Germany), A.P. Sloan Foundation, Civilian Research and Development Foundation, Research Corporation, Texas Advanced Research Program, and the Alexander von Humboldt Foundation.

[1] M.Fischer, S.Groote, J.G.Korner, and M.C.Hauser, Phys. Rev. D **63** 031501 (2001).

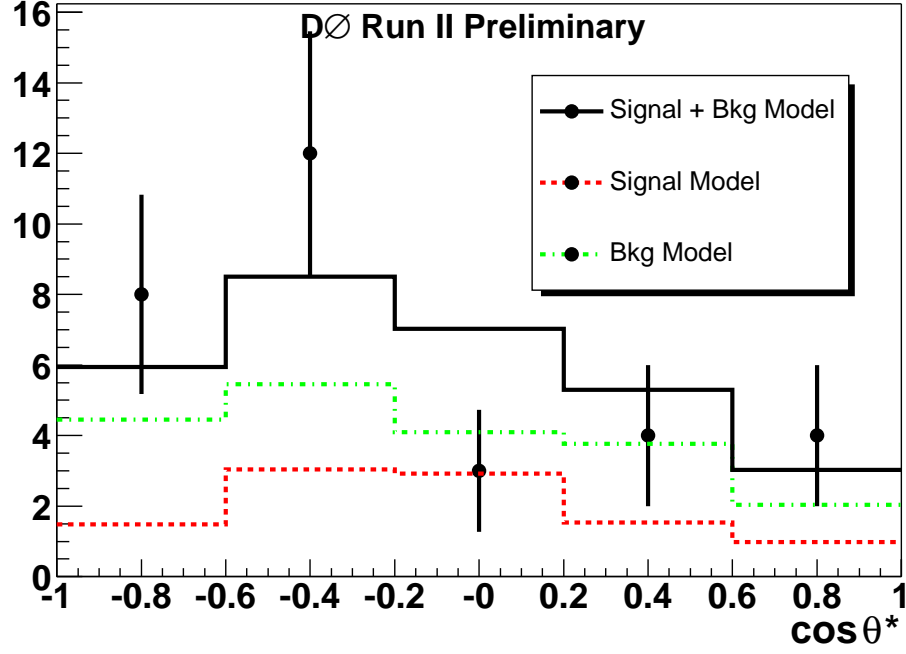


FIG. 6: Comparison of μ +jets data (points with errors bars) to the sum of the best-fit templates of signal and background (solid histogram). The signal and background contributions are shown separately as the dashed and dotted histogram.

- [2] R.H.Dalitz and Gary R. Goldstein, Phys. Rev. D **45**, 1531 (1992).
- [3] CDF Collaboration, T. Affolder *et al.*, Phys. Rev. Lett. **84**, 216 (2000).
- [4] DØ Collaboration, V.M. Abazov *et al.*, hep-ex/0404040 (2004).
- [5] M.F. Canelli, *Helicity of the W in Single-Lepton tt Events*, Ph.D. Thesis, University of Rochester, (2003).
- [6] K. Fujikawa and A. Yamada, Phys. Rev. D **49**, 5890 (1994).
- [7] P. Cho and M. Misiak, Phys. Rev. D **49**, 5894 (1994).
- [8] DØ Note 4423-CONF *Measurement of the tt Production Cross Section at $\sqrt{s} = 1.96$ TeV in the Lepton Plus Jets Final States Using a Topological Method*.
- [9] M.L. Mangano *et al.*, *ALPGEN, a generator for hard multiparton processes in hadronic collisions*, JHEP 0307:001,2003, hep-ph/0206293.
- [10] T. Sjöstrand, *et al.*, Computer Phys. Commun. 135 (2001) 238 (LU TP 00-30, hep-ph/0010017)
- [11] R. Barlow and C. Beeston, Comp. Phys. Comm. **77** 219 (1993).
- [12] G. Feldman and R. Cousins, Phys. Rev. D **57** 3873 (1998).
- [13] DØ Note 4545-CONF *Measurement of the W Helicity in tt Decays at $\sqrt{s} = 1.96$ TeV in the Lepton + Jets Final States Using a Lifetime Tag*

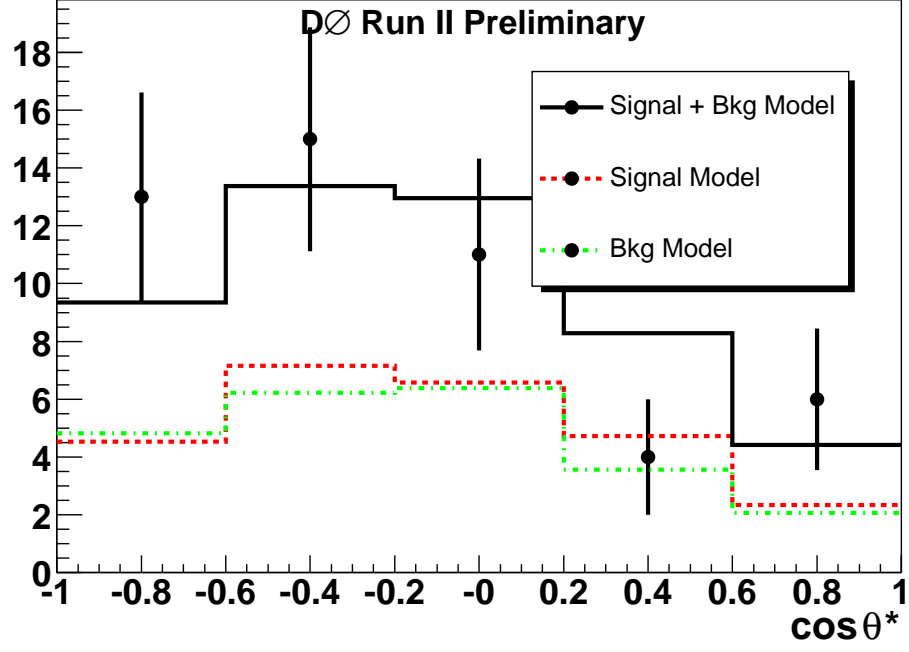


FIG. 7: Comparison of e +jets data (points with errors bars) to the sum of the best-fit templates of signal and background (solid histogram). The signal and background contributions are shown separately as the dashed and dotted histogram.

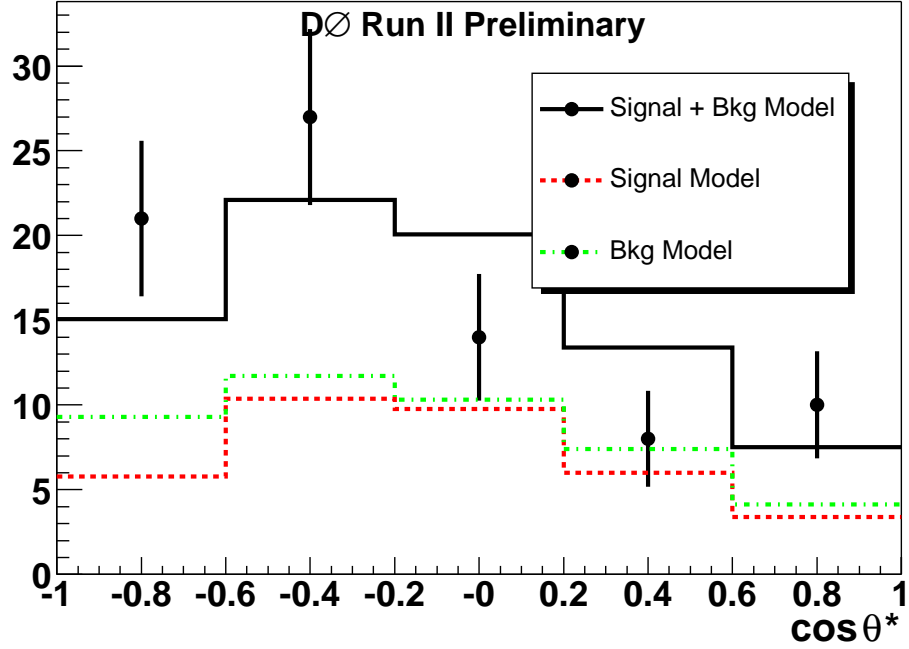


FIG. 8: Comparison of the sum of μ +jets and e +jets data (points with errors bars) to the sum of the best-fit templates of signal and background (solid histogram). The signal and background contributions are shown separately as the dashed and dotted histogram.

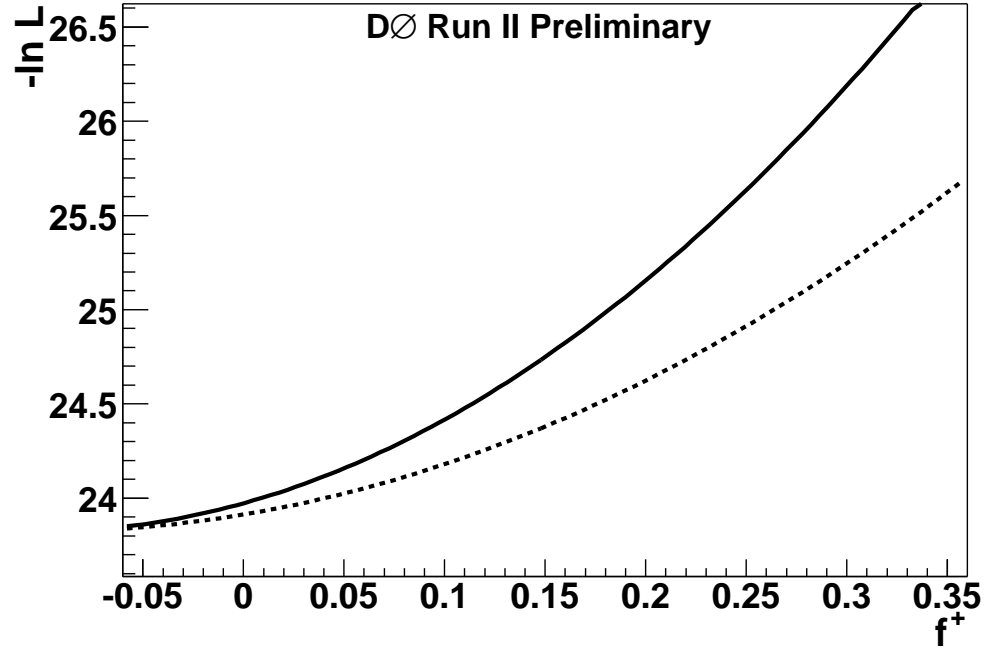


FIG. 9: Results of the combined e +jets and μ +jets maximum likelihood fits including statistical errors only (solid line) and including both statistical and systematic errors (dashed line).